Carbohydrate Polymers 88 (2012) 628–637

Contents lists available at SciVerse ScienceDirect

Carbohydrate Polymers

journal homepage: www.elsevier.com/locate/carbpol

Dielectric behaviour and pore size distribution of collagen–guar gum composites: Effect of guar gum

Reshme Manikoth, Ivy Kanungo, Nishter Nishad Fathima*, Jonnalagadda Raghava Rao

Chemical Laboratory, Central Leather Research Institute, Council of Scientific and Industrial Research, Adyar, Chennai 600020, India

ARTICLE INFO

Article history:
Received 20 October 2011
Received in revised form 3 January 2012
Accepted 3 January 2012
Available online 18 January 2012

Keywords:
Collagen
Guar gum
Circular dichroic spectroscopy
Dielectric
Thermoporometry

ABSTRACT

Collagen is usually combined with other biopolymers to enhance its physico-chemical properties for tissue engineering applications. In this study, guar gum, a non ionic plant derived polysaccharide was mixed with collagen and the effect of the same on dielectric behaviour and pore size distribution of the composites has been investigated. Circular dichroic studies show that guar gum does not bring any alteration in the conformation of the native protein. Thermoporometry result shows that by varying the concentration of guar gum, the pore size distribution of the biocomposite can be controlled. The thermal stability of biocomposite system increases as the concentration of guar gum increases and reaches a maximum of $40 \pm 0.5\,^{\circ}C$. Initiation of the polarization mechanism through the ionic charge drift on the protein-additives interfaces is affected due to the guar gum concentration, which influences the hydration shell of the protein molecule.

1. Introduction

Collagen-based biomaterials are being developed for a number of tissue engineering and medical applications such as sealants, adhesion barriers, and scaffolds (Remi, Robert, & Francois, 2010). Collagen is the most abundant protein in extra cellular matrix, which constitutes about 30% of total body protein (Gelse, Poschl, & Aigner, 2003). Inter-chain hydrogen bonds and structural water molecules play an important role in stabilizing the structure of collagen (Wolfgang, 1998). The attractiveness of collagen as a biomaterial rests largely on the view that it is a natural material of low immunogenicity and is therefore seen by the body as a normal constituent rather than foreign matter (Devore et al., 1995; Gorham, 1991). However, thermal stability of collagen is not sufficient for many in vivo and in vitro applications. In order to render collagen suitable for tissue engineering applications, the mechanical strength of collagen must also be enhanced, which can be achieved through crosslinking using biodegradable polymers (Hubbell, 1995; Laurencin, Ambrosto, Borden, & Cooper, 1999). Biodegradable polymers offer a number of advantages over other materials for developing scaffolds in tissue engineering (Gunatillake & Adhikari, 2003).

Guar gum, an extract from the seeds of *Cyamopsis tetragonolobus*, shows a backbone of β-D-mannopyranoses linked 1→4 to which, on average, every alternate mannose and α-D-galactose is linked 1→6 (Panariello, Favaloro, Forbicioni, Caputo, & Barbucci, 2008). This polymer has proven particularly useful for colon delivery as it can be degraded by the specific enzymes present in this tract of the intestine (Singh & Kim, 2005). It is not affected by ionic strength or pH at moderate temperature due to its non-ionic nature. Because of this property, guar gum can protect the drug in the stomach and small intestine environment, leading to the final delivery of the drug (Rubinstein, 2000). A recent study has also investigated the preparation of disc-shaped matrices of guar for colon specific delivery (Kabir, Yagen, Penhasi, & Rubinstein, 1998). By introducing modifications on the polymeric chain of guar, the dosage forms were prepared capable of carrying their hydrophobic drug load through the proximal portions of the GI tract, while maintaining their susceptibility to degradation by the colonic enzymes (Das, Wadhwa, & Srivastava, 2006). Recent pyro and piezoelectric studies of galactomannan crosslinked with collagen films showed the presence of natural polarity in the structure of galactomannan–collagen based biomaterials (Figueiro, Julio, Moreira, & Sombra, 2004).Although few studies on collagen–guar gum interaction have been carried out, the influence of guar gum on various properties of collagen like pore size distribution, dielectric behaviour, thermal stability and conformational change have not been addressed yet. Properties like dielectric (Bettinger, Bruggeman, Misra, Borenstein, & Langer, 2009), thermal stability (Ohya & Matsuda, 2005) and pore size (Obriena, Harley, Yannas, & Gibson, 2005) have a great influence on the designing of engineered biomaterials. In this study, the effect of guar gum on physico-chemical property of collagen has been studied using techniques such as thermoporometry, differential scanning

* Corresponding author. Tel.: +91 44 24411630; fax: +91 44 24911589.
E-mail addresses: nishad.naveed@gmail.com, nishad@clri.res.in (N.N. Fathima).

0144-8617/$ – see front matter © 2012 Elsevier Ltd. All rights reserved.
doi:10.1016/j.carbpol.2012.01.031

calorimetry (DSC), scanning electron microscopy (SEM), viscosity, circular dichroism (CD), attenuated total reflectance-Fourier transform infrared spectroscopy (ATR-FTIR) and dielectric spectroscopy. Thermoporometry technique has been found to be a useful tool for studying the pore size distribution of biological materials in native state using Gibbs–Helmholtz equation (Fathima, Baias, Blumich, & Ramasami, 2010; Fathima, Pradeepkumar, Rao, & Nair, 2010). The drug release is governed by pore size, which confines the space of drug or amount of drug that can be loaded. Depending on pore size distribution sustained or controlled release of loaded drug can be obtained (Barbani et al., 1995). Dielectric spectroscopy offers insights into the dynamic and structural properties of biopolymers. It is very sensitive and helps in monitoring interface polarization and intermolecular (dipole–dipole) interaction of bio-molecules (Friess & Lee, 1996; Marzec & Warchol, 2005; Samouillan, Lamure, & Lacabanne, 2000; Samouillan, Lamure, Maurel, et al., 2000). This study investigates the influence of guar gum on the average pore diameter and pore size distribution of collagen based biocomposite as well as the effect of the same on hydration of collagen molecule. The objective is to design a suitable biocomposite based on collagen for biomedical applications.

2. Experimental techniques

2.1. Materials

Guar gum was purchased from SD Fine Chemicals Ltd., India. Tails were excised from 6-month-old male albino rats (Wistar strain) and frozen at −20 °C. On removal from the freezer, tails were thawed and tendons were teased out. Teased collagen fibres were washed with 0.9% NaCl at 4 °C, to remove the adhering soluble proteins. Acid soluble rat tail tendon type I collagen was isolated according to the method described by Chandrakasan, Torchia, and Piez (1976). The procedure includes acetic acid extraction and salting out with NaCl. The purity of collagen was confirmed by SDS-polyacrylamide gel electrophoresis (gel has been shown as supplementary data). The collagen concentration in the solutions was determined from the hydroxyproline content according to the method of Woessner (1961).

2.2. Composite preparation

0.5% (w/v) guar gum was prepared by continuous stirring for 1 h at 50 °C. The aqueous solution was filtered using Qualigens 615A filter paper of circles 100, dia. 15 cm, and medium fast filter speed. The aqueous solution of collagen–guar gum composites was prepared at the different molar concentration ratios (1:1, 1:10, 1:20, 1:40, and 1:50) with fixed concentration of collagen (0.404 μM) at pH 4.5. The temperature was maintained at 4 °C. Samples for SEM and FTIR analysis were lyophilized under the pressure of 6.4 Pa at −40 °C to get a sponge like material. Prior to lyophilization, all the composites were frozen by dipping in liquid nitrogen and kept in deep-freezer overnight. All other characterizations were carried out in liquid state.

2.3. Characterization of the composite systems

2.3.1. Viscosity measurement

The viscosity of the composites was measured using Ostwald type viscometer of 2 ml capacity. The viscometer was thermostated at 25 °C. The flow times of buffer, protein solution, protein solution with additives at the different molar concentration ratios of 1:1, 1:10, 1:20, 1:40, and 1:50 with fixed concentration of collagen (0.404 μM) were measured in triplets with a digital stopwatch after a thermal equilibrium time of 15 min for the estimation of the effect of guar gum concentration on the absolute viscosity of protein. The average was taken. The viscosity (η) of collagen was measured as a function of additive concentration. The viscosity was calculated from the relation,

$$\text{Specific viscosity, } \eta_{sp} = \frac{t - t_0}{t_0} \quad (1)$$

where t_0 is the flow time of buffer and t is the flow time for each sample.

$$\text{Relative viscosity, } \eta_{relative} = \frac{\eta}{\eta_0} \quad (2)$$

$\eta_{relative}$ (where η and η_0 are the viscosity of collagen in the presence and absence of guar gum) was plotted with $1/R$ (R = [collagen]/[guar gum]).

2.3.2. Circular dichroism (CD) spectroscopic studies

Circular dichroic spectra were measured using a Jasco 815 Circular Dichroism spectropolarimeter using a quartz cell with a light path of 1 mm at 0.2 nm intervals, at 25 °C, with 2 scans averaged for each sample. CD spectra were recorded to estimate the conformational changes of collagen when treated with guar gum in the far UV region (190–250 nm), using constant nitrogen flow rate. The data were plotted as mean-residue-weight ellipticity (deg. cm^2 $dmol^{-1}$) versus wavelength in nm. An aqueous solution of collagen (0.404×10^{-6} M) in acetate buffer (pH 4.0, 1×10^{-2} M) was treated with the guar gum (0.404×10^{-6} to 20.2×10^{-6} M) and incubated for 1 h at 4 °C. Effect of guar gum on the thermal stability of collagen was measured between temperatures from 35 to 40 °C with an interval of 0.5 °C. The melting temperature of collagen is 37 °C (Fathima, Balaraman, Rao, & Nair, 2003), hence to study the influence of guar gum on thermal stability of collagen a lower side temperature of 35 °C was chosen. The higher temperature was fixed as 40 °C, as complete denaturation occurred at that temperature for maximum concentration of guar gum.

2.3.3. Thermoporometric studies for pore size distribution

Thermoporometric analysis was carried out using TA Instruments Q200 Differential Scanning Calorimeter (DSC), USA. Prior to measurement, the sample loaded in hermetically encapsulated aluminium pan was cooled to −40 °C and held at that temperature for 30 min. All measurements were carried out between −40 and 10 °C with a scan rate 1 °C/min. All measurements were performed in triplets. The peak temperature (T_m) and total enthalpy (ΔH_m) for the transition was obtained using the system generated software. Pore size distribution was determined by measuring the amount of water that has its melting temperature depressed at each step (Fathima, Baias, et al., 2010; Fathima, Pradeepkumar, et al., 2010). The enthalpies ($H_1, H_2, H_3, \ldots, H_i$ J/g) obtained from the DSC is noted to the corresponding temperatures (T_1, T_2, T_3, …, T_i °C) with step size 0.1 K. The pore radius is calculated as per Eq. (3)

$$R_p = -\frac{32.33}{\Delta T} + 0.68 \quad (3)$$

where R_p is the pore radius, and $\Delta T = T - T_0$ the triple point depression, with T_0 being the triple point temperature of the solvent.

For corresponding pore radius R_p, the average temperature interval T'_i is calculated as per Eq. (4)

$$T'_i = \frac{T_i + T_{i+1}}{2} \quad (4)$$

The volumic latent heat W_V (J/cm^3) is derived by the following correlation between specific latent heat of fusion W_S (J/g) and specific volume of solvent V (cm^3/g) as per Eq. (5)

$$W_V = \frac{W_S}{V} \quad (5)$$

where $W_S = -(0.0556(T'_i - T_0)^2 - 11.39(T'_i - T_0) - 332)$ and $V = 1.000132(1 - 0.000091T'_i + (1.035 \times 10^{-5})T_i^2)$.

Pore volume ΔV is further calculated as follows,

$$\Delta V = \frac{S_i}{W_V \times M \times 1000} \quad (6)$$

where M is the mass of dry sample in grams.

Pore volume distribution was further derived by using the equation,

$$\frac{dV}{dR_p} = \frac{\Delta V}{T_i - T_{i+1}} \quad (7)$$

2.3.4. Attenuated total reflectance-Fourier transform Infrared (ATR-FTIR) spectroscopic characterization

Attenuated total reflectance-Fourier transform infrared spectroscopic measurements performed by ABB MB 3000 instruments (Pike Technologies, USA) determine the change in the functional group of protein when treated with guar gum. Each measurement included 60 double-sided scans in the 600–4000 cm^{-1} range, with a resolution of 2 cm^{-1}. A background measurement (air) was recorded immediately before each measurement, and the interferogram was transformed into an ATR spectrum using the software operating the spectrophotometer (HORIZON MB^{TM} FTIR).

2.3.5. Scanning electron microscopic (SEM) characterization

Examination of the fracture surfaces was performed on a Hitachi S-3400 (Japan) scanning electron microscope at 10 kV. The fracture ends of the specimens were sputter coated with a thin layer of gold prior to examination.

2.3.6. Admittance measurements

Impedance measurements were carried out at 25 °C using CH instrumental (USA) CH model 660B electrochemical analyser with a classical three-electrode system, where the glassy carbon electrode was used as a working electrode, a platinum electrode as a counter electrode and a saturated calomel electrode as the reference electrode. The operating conditions were init. E (V) = 0.09, high frequency (Hz) = 1e+5, low frequency (Hz) = 0.01, amplitude (V) = 0.005, quiet time (s) = 2, cycles (0.1–1 Hz) = 1, cycles (0.01–0.1 Hz) = 1, cycles (0.001–0.01 Hz) = 1.

Dielectric data can be represented in terms of admittance or permittivity. The admittance is a conjugate quantity and may be written as,

$$Y^* = Y' - jY'' \quad (8)$$

where Y' is the real component describing the energy stored and Y'' is the imaginary component depicting the energy dissipated by the system.

3. Results and discussions

3.1. Changes in rheological behaviour of collagen on interaction with guar gum

In order to understand the guar gum–collagen interaction, the influence of guar gum on the viscosity of collagen was studied. Relative viscosity was measured for collagen in the presence of varying concentrations of guar gum. A plot of relative viscosity (η/η_0) against $1/R$ (R = [collagen]/[guar gum]) shown in Fig. 1 indicates an increase in relative viscosity of collagen with increasing concentration of guar gum. Increase in viscosity of protein is generally attributed to the aggregation of the protein with the additive (Fathima et al., 2003). Hence, guar gum interaction with collagen molecules results in increased viscosity and higher gel integrity.

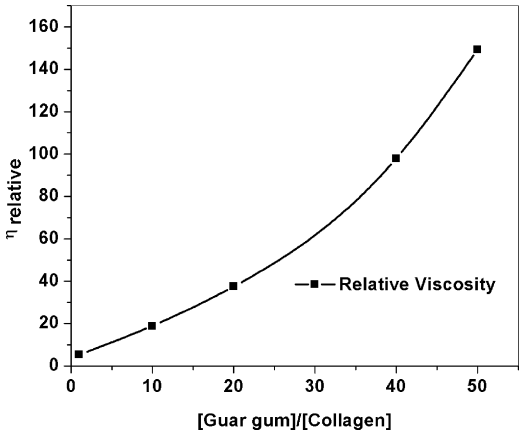

Fig. 1. A plot of relative viscosity (η/η_0) against $1/R$ (η and η_0 are the viscosity of collagen in the presence and absence of guar gum). R = [collagen]/[guar gum]. Temperature = 25 ± 1 °C.

Higher gel integrity could retard diffusion of drug for extended time thus facilitating sustained or controlled release profile.

3.2. Changes in conformation of collagen on interaction with guar gum

Alteration in the secondary structure of collagen due to interaction with guar gum was investigated by circular dichroic spectroscopic studies. The triple helical conformation of collagen gives a CD spectrum characterized by a positive peak at 220 nm and a negative peak at 197 nm (Fathima, Bose, Rao, & Nair, 2006). Fig. 2 shows the far UV-CD spectra of collagen in the presence of guar gum at different ratios. Only minor changes in the molar ellipticity values could be seen. Collagen on denaturation leads to red shift of negative band (Fathima et al., 2003). No such effects were observed in guar gum treated composites. Thus, it can be inferred that collagen secondary structure is maintained even at higher guar gum concentration. The parameter R_{pn}, a characteristic ratio for the triple helical conformation of collagen and collagen like peptide, denotes the ratio of positive peak intensity over negative peak intensity (Brown, Corato, Lorenzi, & Blout, 1972; Feng, Melacini, Taulene, & Goodman, 1996). The R_{pn} value of native collagen was found to be 0.118 where as the values are 0.119, 0.119, 0.121, 0.121, and 0.121 for collagen–guar gum composites with the increasing guar gum concentration (Table 1).

The effect of guar gum on the thermal stability of collagen was monitored by temperature dependant circular dichroism

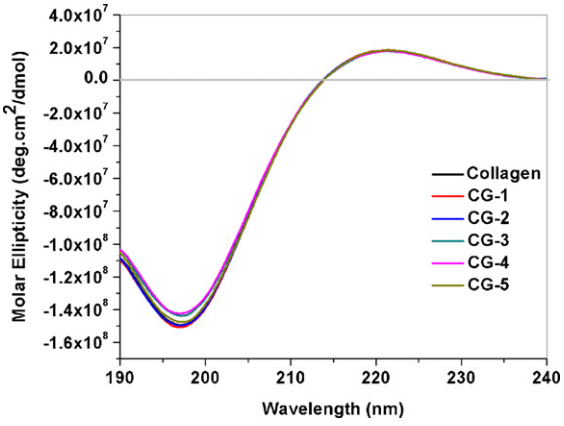

Fig. 2. Far-UV CD spectra of collagen in the presence of different guar gum concentration. [collagen] = 0.404 μM:[guar gum] = 0.404–20.2 μM. Temperature = 25 °C.

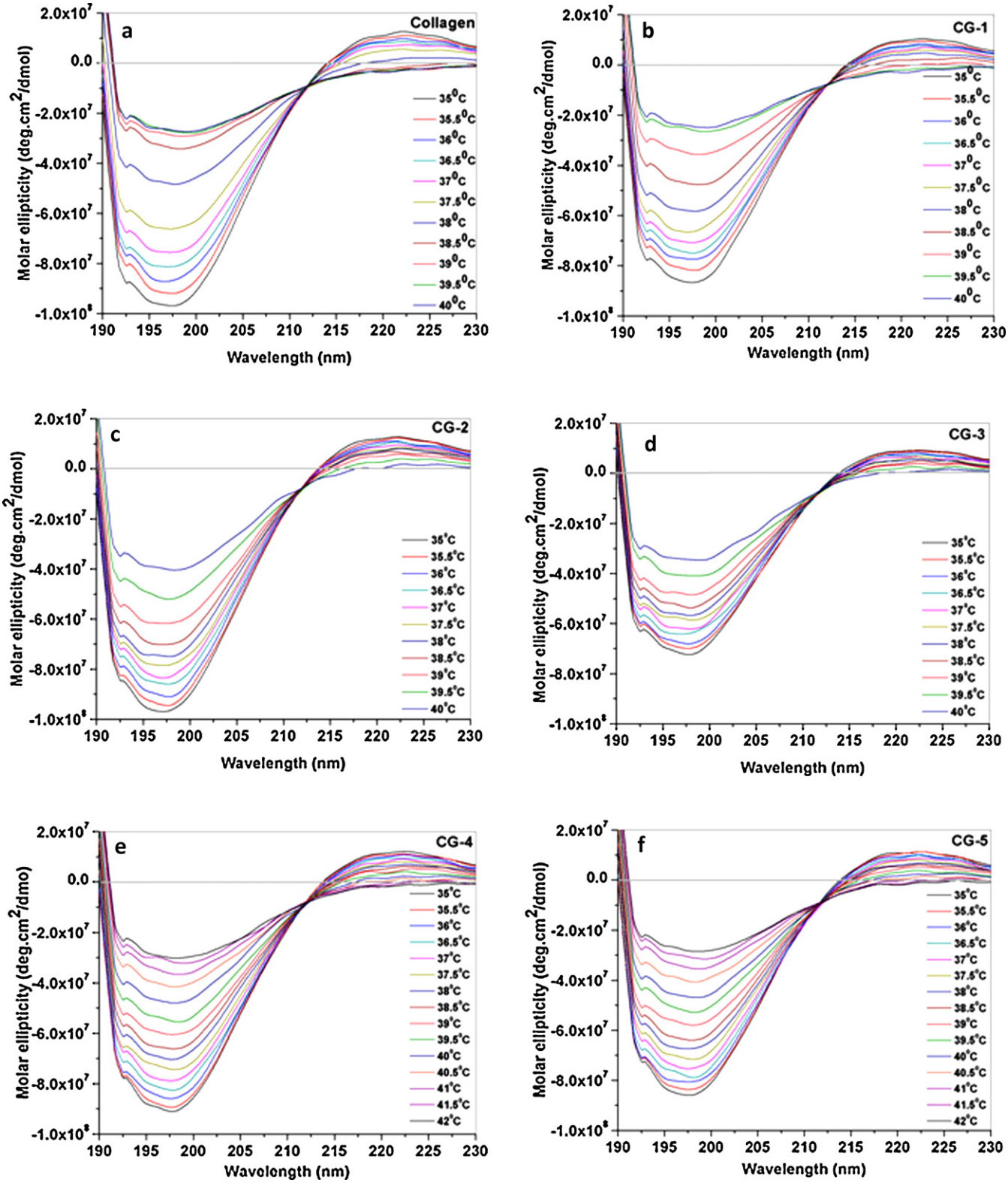

Fig. 3. Temperature dependent CD-spectra for collagen–guar gum composites. [collagen] = 0.404 μM:[guar gum] = 0.404–20.2 μM. Temperature = 30–42 °C, rate of increase of temperature = 0.5 °C/min.

spectroscopic studies. Fig. 3(a)–(f) shows the far UV-CD spectra of collagen in the presence of guar gum at different ratios. It can be seen from Fig. 3(a) that native collagen gets denatured at a temperature of 37 °C. Fig. 3(b)–(f) shows that as the concentration of guar gum increases in the composite system, the denaturation temperature also increases to about 40 ± 0.5 °C (8% increase), which denotes that there is increase in the thermal stability of collagen on interaction with guar gum. It is evident from the above studies

Table 1
R_{pn} ratio for native collagen and collagen–guar gum composites at different temperatures (CG = collagen:guar gum molar ratios 1:1 to 1:50).

Temperature	R_{pn}					
	Collagen	CG-1	CG-2	CG-3	CG-4	CG-5
35.0	0.113	0.110	0.122	0.122	0.125	0.125
35.5	0.109	0.109	0.118	0.119	0.119	0.124
36.0	0.099	0.095	0.115	0.111	0.114	0.114
36.5	0.098	0.092	0.108	0.109	0.112	0.110
37.0	0.089	0.081	0.103	0.102	0.098	0.104
37.5	0.073	0.075	0.094	0.091	0.097	0.106
38.0	0.017	0.068	0.091	0.085	0.089	0.086
38.5	0.073	0.039	0.088	0.069	0.076	0.082
39.0	0.114	0.014	0.079	0.066	0.062	0.075
39.5	0.115	0.077	0.049	0.044	0.055	0.058
40.0	0.140	0.125	0.005	0.017	0.030	0.034
40.5	–	–	–	–	0.004	0.008
41.0	–	–	–	–	0.026	0.015
41.5	–	–	–	–	0.062	0.056
42.0	–	–	–	–	0.061	0.074

that addition of guar gum not only retains the native structure of collagen but also leads to improvement in the thermal stability of collagen due to hydrogen bonded interactions.

3.3. Changes in pore size distribution of collagen on interaction with guar gum

Pore size and pore network of a biomaterial influences the drug delivery process significantly (Obriena et al., 2005). Thermoporometry technique unlike other porosimetry techniques measures the pore size distribution of the samples in their wet native state (Fathima, Dhathathreyan, & Ramasami, 2002, 2007). The phase transitions (crystallization or melting) of a liquid confined within a pore are observed to shift to lower temperatures due to different thermodynamic behaviour from unbound water and are characterized by integration of the endotherm (Hori, Zhang, & Shimizu, 1988; Yamauchi & Murakami, 1991). The thermoporometric investigation on collagen–guar gum composites reveals significant variations in pore size distribution with the various concentration of guar gum. Fig. 4(a)–(g) shows the pore size distribution of collagen–guar gum composites. Fig. 4(a) indicates the pore size distribution of native collagen ranging from 3 to 70 nm where as for guar gum, pore size distribution shown in Fig. 4(b) varies from 2 to 50 nm. Large numbers of pores are present both for the native protein as well as guar gum. The influence of different guar gum concentration on the pore size distribution of the composites is shown in Fig. 4(c)–(g). As the concentration of guar gum increases, pore sizes are shifted to the lower nanometer range and pore population also decreases. Hence, it can be concluded that there is a significant influence of composition on the pore size distribution of composite, which in turn can influence the properties of biomaterial intended for tissue engineering applications (Murphy, Haugh, & O'Brien, 2010; Van Tienen et al., 2002; Wake, Patrick, & Mikos, 1994). The average pore diameter of these chemical analogs of extracellular matrices were restricted between 20 and 125 μm to be morpho-genetically active (Van Tienen et al., 2002). Porous implants with the minimum pore size for significant bone growth is 75–100 μm with an optimal range of 100–135 μm where as for skin regeneration the critical range of pore size is 20–120 μm (Murphy et al., 2010). All types of composites had a favourable pore structure to facilitate the cell growth for the wound healing.

3.4. Changes in the functional group of collagen on interaction with guar gum

The IR spectroscopic method is frequently used to investigate the interaction between two polymers. The sensitive characteristic absorption bands of collagen on the IR spectrum were located in spectral regions of amide I, amide II and amide III. In Fig. 5(a) the characteristic peaks of collagen appears at 3312 cm^{-1} (amide A, N—H stretching and O—H stretching), 2930 cm^{-1} (amide B, C—H stretching), 1642 cm^{-1} (amide I, C=O stretching), 1555 cm^{-1} (amide II, N—H bending and C—N stretching), 1243 cm^{-1} (amide III, CN stretching and N—H bending), and 1068 cm^{-1} (bend of carboxyl OH) (Chen, Wang, Wec, Mo, & Cui, 2010). In Fig. 5(b) the characteristic peak of guar gum appears at 871 cm^{-1} (galactose and mannose units) and 930–770 cm^{-1} (1–4, 1–6 linkage of galactose and mannose) (Rana et al., 2010). Fig. 5(c)–(g) shows the interaction of collagen–guar gum composites.

The strong interactions are evidenced in Fig. 5(c)–(g) by the shift of peaks or in peak duplications. Shifts of amide I band from 1641 cm^{-1} to 1650 cm^{-1} and shifts of carboxyl OH bend from 1068 cm^{-1} to 1024 cm^{-1} of collagen–guar gum composites spectra have been observed. Amide I band in ATR-FTIR spectra of collagen is sensitive to secondary structure of collagen (Kaminska & Sionkowska, 1996; Sionkowska, 2000). Unchanged position of amide I of collagen in the composites clarified the unchanged secondary structure of collagen in the composites, which is in coherence with the CD results. It confirms that the triple helical structure of collagen is unchanged during the formation of collagen–guar gum composites. The frequency of the CO stretching of the Amide I band is sensitive to the environment, as well as on the coupling with other modes. The small variation in the frequency of amide I indicates the change in the surroundings of CO, which in turn indicates the change in hydration dynamics of CO groups. Each type of secondary structure gives rise to a somewhat different C=O stretching frequency due to unique molecular geometry and hydrogen bonding pattern. This can lead to change in hydrodynamic radius of the protein and hence the pore size of the composite.

3.5. Changes in morphology of collagen on interaction with guar gum

Scanning electron microscopy studies were carried out to investigate the effect of guar gum on the morphology of collagen. Fig. 6(a)–(g) shows the SEM micrographs of native collagen, guar gum and collagen–guar gum scaffolds at a magnification of 2000×. Each composite shows different surface morphology. Collagen and guar gum show fibillar structure and as the concentration of guar gum differs the morphology also changes. They formed a film like scaffold. This shows that there is an interaction between collagen and guar gum, which causes alterations in the morphology.

3.6. Changes in hydration of collagen on interaction with guar gum

The electrostatic van-der-Waals interactions exist between the molecules at the interface. In the dielectric method, the amino acids through the carbonyl group get absorbed to the electrode surface and the positively charged surface facilitates the interaction with negatively charged carboxyl group. The change in the dielectric behaviour of collagen on interaction with guar gum has been plotted as the Nyquist plot (Fig. 7(a)) and Bode plot (shown in Fig. 7(b)).

Polar molecules are reoriented in presence of an external electric field contributing to the dielectric relaxation. Dielectric dispersion over a frequency range (distinguished by three dispersions called α, β, γ) shown in Fig. 7(b) is caused by charge organization onto the interfaces of the biological macromolecule in presence of water molecule and hydrated ions due to its hindered vibrational and rotational mobility. The degree of hydration is affected by the

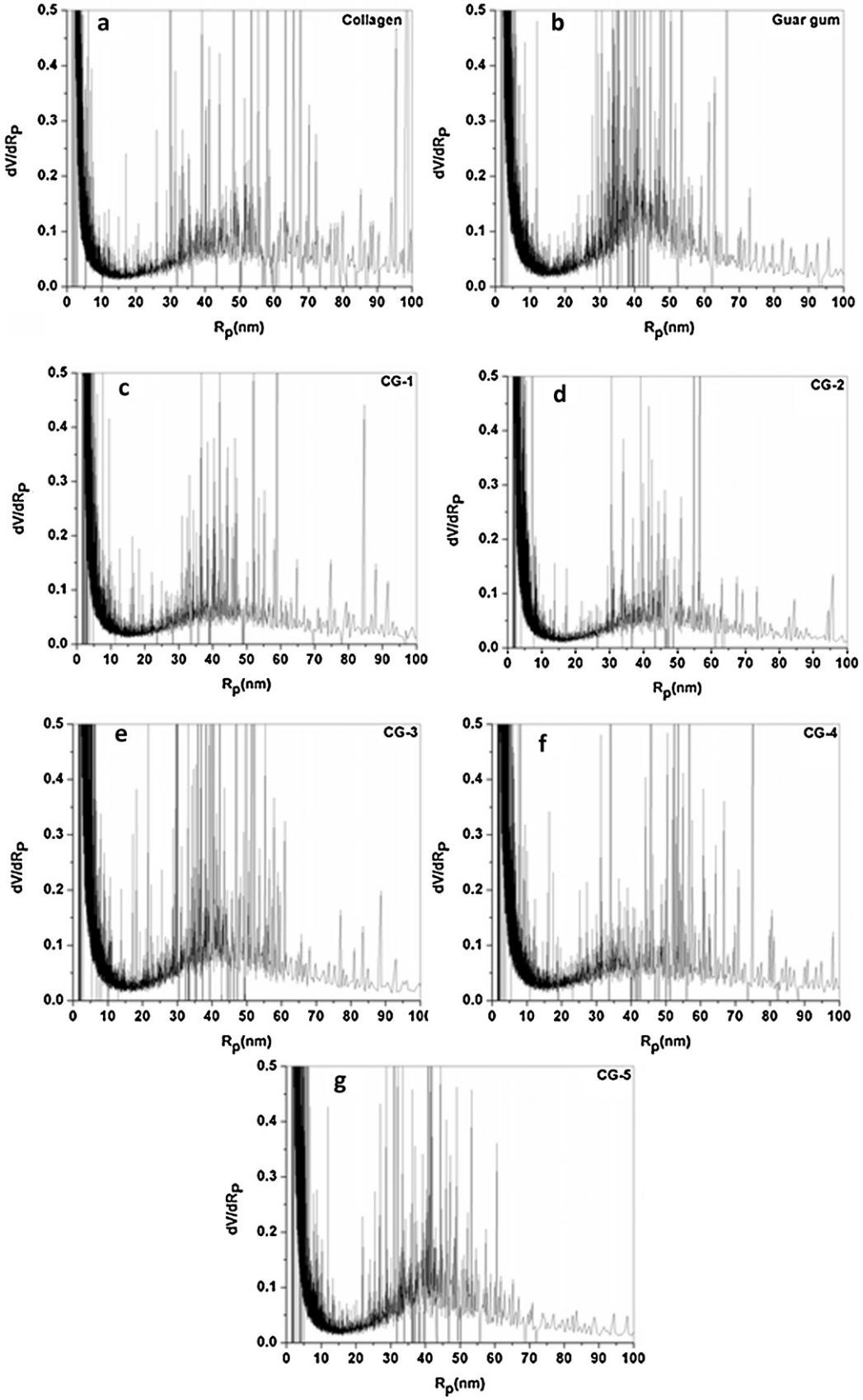

Fig. 4. Pore size distribution of collagen, guar gum and collagen–guar gum composites. [collagen] = 0.404 μM:[guar gum] = 0.404–20.2 μM. Temperature = −40 to 10 °C, rate of increase of temperature = 1 °C/min.

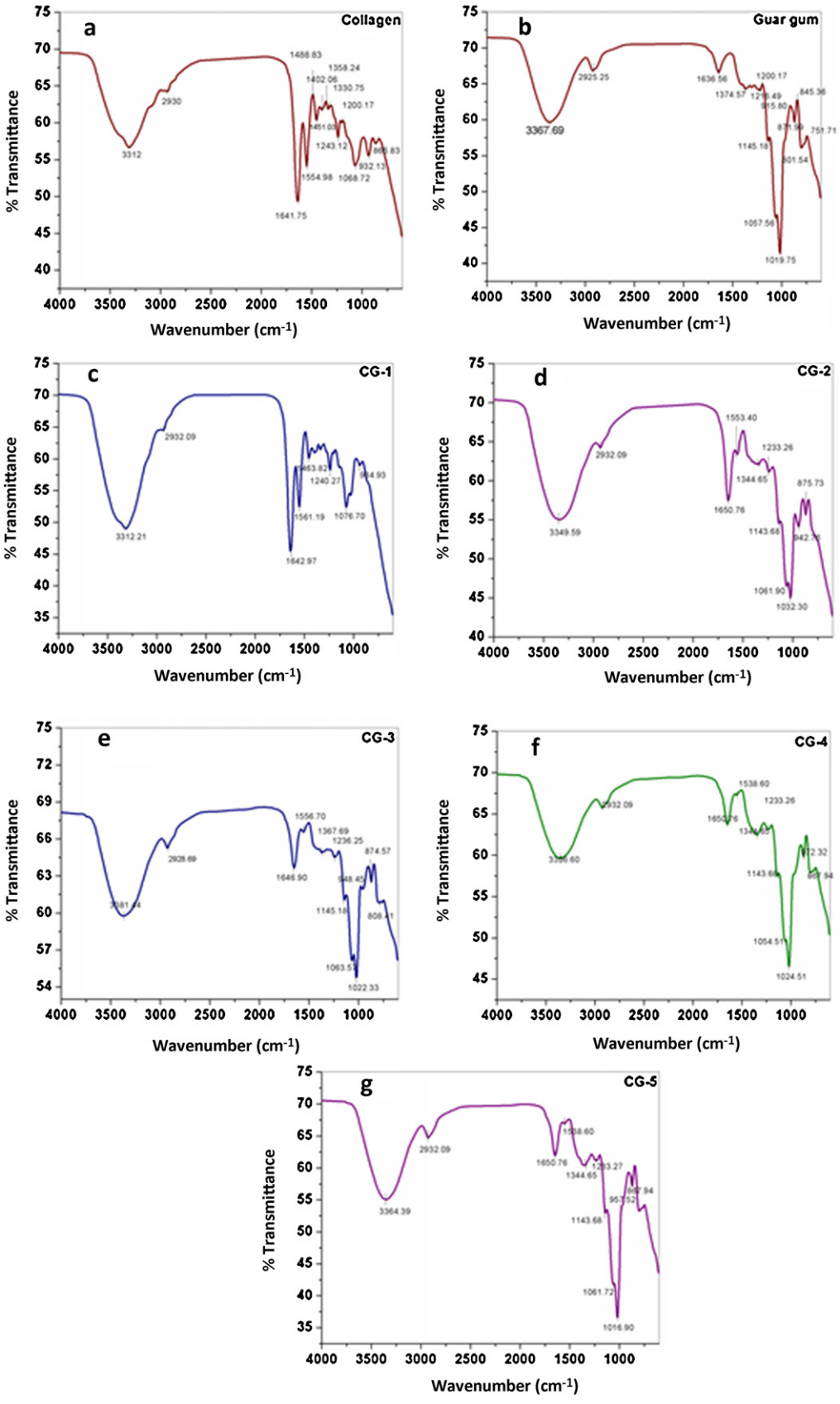

Fig. 5. ATR-FTIR spectra of collagen–guar gum composites. [collagen] = 0.404 μM:[guar gum] = 0.404–20.2 μM.

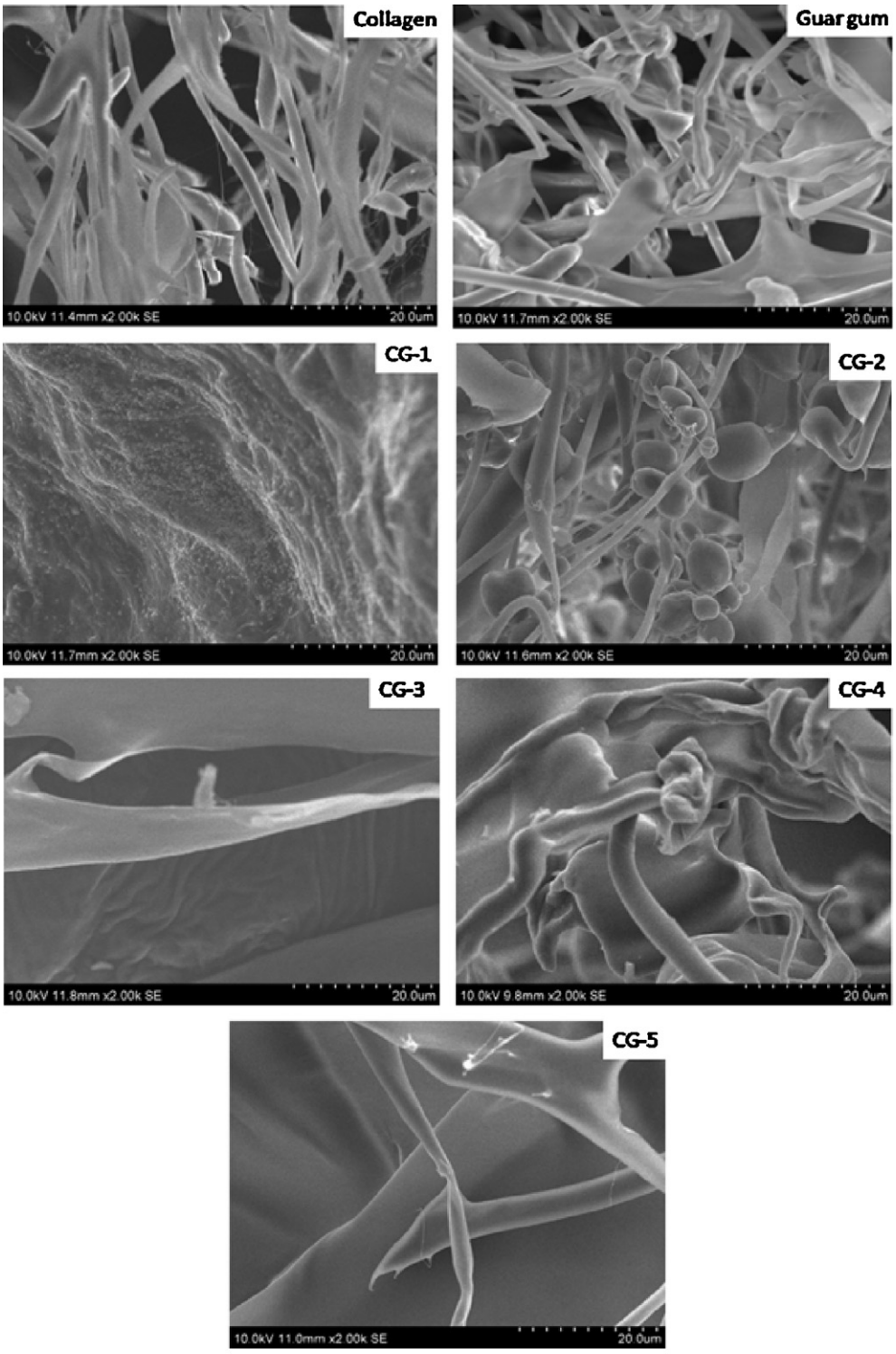

Fig. 6. SEM micrographs of native collagen, native guar gum and different collagen–guar gum composites.

strength of ion pairs present in between the amino groups and carboxyl groups of protein as well as other polar molecules (Marion, Monica, & Muller, 2008; Pethig & Kell, 1987). α dispersion, observed at below few kHz, results due to ionic diffusion process whereas β dispersion in the hundreds of kHz region arises from interfacial polarization. γ dispersion is the result of the polarization of bulk water molecules in the solution. These dielectric mechanisms can cause a variation in permittivity. At the pH 4.5, collagen carries the net positive charges on its triple helical structure. Although the charge nature of the collagen is unaffected after complexation with non ionic guar gum, the hydration shell of the protein molecule is tuned with the guar gum concentration. Decrease in permittivity (i.e. admittance) with increase of guar gum concentration indicates the alteration of polarizability of functional groups which in turn destroy the dipolar nature of protein molecule. This explains that the hydration state of the interface changes when protein adsorbs onto the surface or interacts with guar gum.

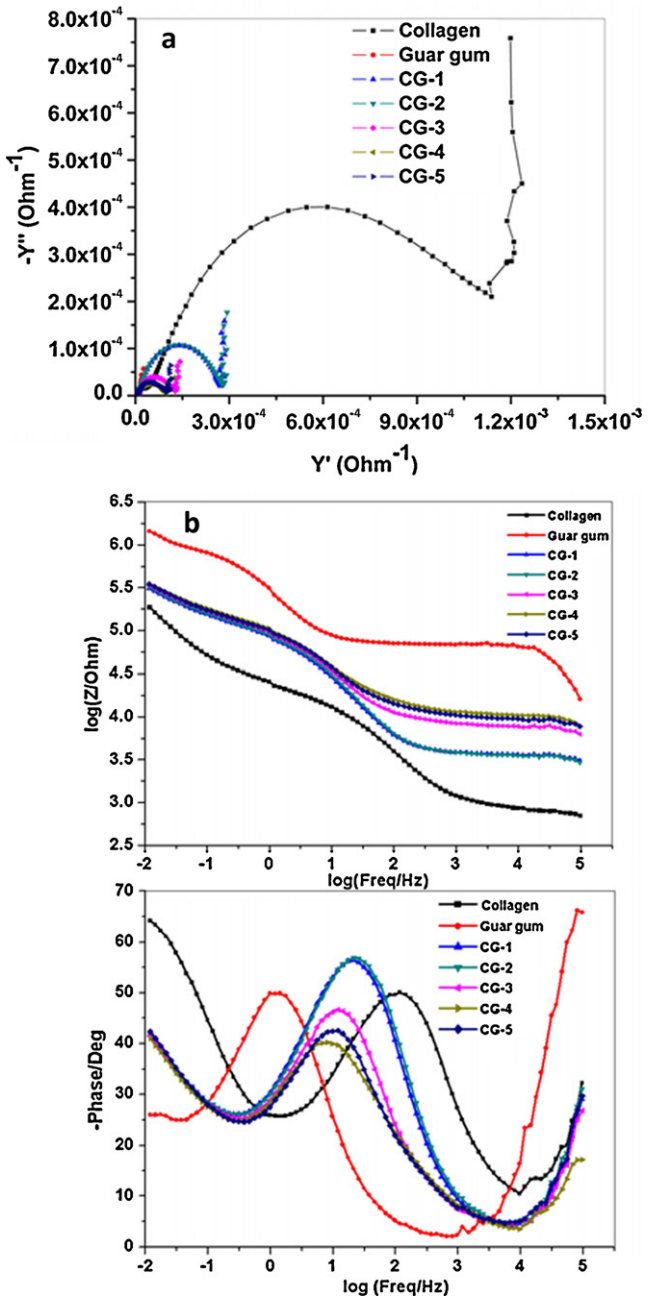

Fig. 7. (a) Nyquist plot for Faradaic admittance measurement. (b) Bode plot for dielectric dispersion behaviour. [collagen] = 0.404 μM:[guar gum] = 0.404–20.2 μM, temperature = 25 °C.

4. Conclusions

In the present work, the effect of guar gum on the thermal stability, dielectric property and pore size distribution of collagen based biocomposite has been studied. Guar gum causes changes in the rheological properties of the collagen with no effect on the native protein structure as evidenced from CD studies. The different concentration of guar gum resulted in four distinct composites with different mean pore diameters and distribution. Each composite had a consistent pore structure and showed no obvious variation in mean pore size, structure, or alignment at separate points within the composites, indicating the homogeneity of composites produced. The pore size distribution of the biocomposite matrices can be shifted to the lower nanometer range by varying the guar gum concentration. Homogeneity of the pore sizes was increased with the increase of guar gum concentration. Composites with smaller pores have a greater surface area which influences ligand–integrin interaction facilitating the initial cellular attachment. Changes in functional group and morphology of composites indicate that collagen interacts with guar gum chemically and physically. Increase in concentration of guar gum results in increase in thermal stability. The polarizability of the collagen is tuned by the guar gum concentration. Ionic charge drift creates conduction currents and also initiates polarization mechanisms through charge accumulation at structural interfaces. Their dielectric properties reflect contributions to the polarization from both structure and composition of the designed biomaterial. Behavioural changes of the rotational as well vibrational motion of the polar functional groups associated with the protein are due to the formation of hydrogen bond between functional groups of protein and guar gum. This leads to the alteration of the hydration shell of the collagen. This study highlights that composites with variable pore sizes optimal for cell growth can be achieved by varying the guar gum concentration, which can be used for biomedical applications.

Appendix A. Supplementary data

Supplementary data associated with this article can be found, in the online version, at doi:10.1016/j.carbpol.2012.01.031.

References

Barbani, N., Cascone, M. G., Giusti, P., Lazzeri, L., Polacco, G., & Pizzirani, G. J. (1995). Bioartificial materials based on collagen. 2. Mixtures of soluble collagen and poly (vinyl alcohol) cross-linked with gaseous glutaraldehyde. *Journal of Biomaterial Science Polymer Edition*, *7*, 471–484.

Bettinger, C. J., Bruggeman, J. P., Misra, A., Borenstein, J. T., & Langer, R. (2009). Biocompatibility of biodegradable semiconducting melanin films for nerve tissue engineering. *Biomaterials*, *30*, 3050–3057.

Brown, F. R., Corato, A. D., Lorenzi, G. P., & Blout, E. R. (1972). The collagen-like triple helix to random-chain transition: Experiment and theory. *Journal of Molecular Biology*, *63*, 85–99.

Chandrakasan, G., Torchia, D. A., & Piez, K. A. (1976). Preparation of intact monomeric collagen from rat tail tendon and skin and the structure of the non helical ends in solution. *Journal of Biological Chemistry*, *251*, 6062–6067.

Chen, Z. G., Wang, P. W., Wec, B., Mo, X. M., & Cui, F. Z. (2010). Electrospun collagen–chitosan nanofibers: A biomimetic extracellular matrix for endothelial cell and smooth muscle cell. *Acta Biomaterialia*, *6*, 372–382.

Das, A., Wadhwa, S., & Srivastava, A. (2006). Cross-linked guar gum hydrogel discs for colon-specific delivery of ibuprofen: Formulation and in vitro evaluation. *Drug Delivery*, *13*, 139–142.

Devore, D. P., Wise, D. L., Trantolo, D. J., Altobelli, D. E., Yaszemski, M. J., Gresser, J. D., et al. (1995). *Collagen as an ophthalmic biomaterial. Encyclopedic handbook of biomaterials and bioengineering*. New York: Marcel Dekkar., pp. 1233–1260

Fathima, N. N., Baias, M., Blumich, B., & Ramasami, T. (2010). Structure and dynamics of water in native and tanned collagen fibers: Effect of crosslinking. *International Journal of Biological Macromolecules*, *47*, 590–596.

Fathima, N. N., Balaraman, M., Rao, J. R., & Nair, B. U. (2003). Effect of zirconium (IV) complexes on the thermal and enzymatic stability of type I collagen. *Journal of Inorganic Biochemistry*, *95*, 47–54.

Fathima, N. N., Bose, M. C., Rao, J. R., & Nair, B. U. (2006). Stabilization of type I collagen against collagenases (type I) and thermal degradation using iron complex. *Journal of Inorganic Biochemistry*, *100*(11), 1774–1780.

Fathima, N. N., Dhathathreyan, A., & Ramasami, T. (2002). Mercury intrusion porosimetry, nitrogen adsorption, and scanning electron microscopy analysis of pores in skin. *Biomacromolecules*, *3*, 899–904.

Fathima, N. N., Dhathathreyan, A., & Ramasami, T. (2007). Influence of crosslinking agents on the pore structure of skin. *Colloids and Surfaces B: Biointerfaces*, *57*, 118–123.

Fathima, N. N., Pradeepkumar, M., Rao, J. R., & Nair, B. U. (2010). A DSC investigation on the changes in pore structure of skin during leather processing. *Thermochimica Acta*, *501*, 98–102.

Feng, Y., Melacini, G., Taulene, J. P., & Goodman, M. (1996). Acetyl-terminated and template-assembled collagen-based polypeptides composed of Gly–Pro–Hyp sequences. 2. Synthesis and conformational analysis by circular dichroism, ultraviolet absorbance, and optical rotation. *Journal of American Chemical Society*, *118*, 10351–10360.

Figueiro, S. D., Julio, C. G., Moreira, R. A., & Sombra, A. S. B. (2004). On the physico-chemical and dielectric properties of glutaraldehyde crosslinked galactomannan–collagen films. *Carbohydrate Polymers*, *56*, 313–320.

Friess, W., & Lee, G. (1996). Basic thermoanalytical studies of insoluble collagen matrices. *Biomaterials*, *17*, 2289–2294.

Gelse, K., Poschl, E., & Aigner, T. (2003). Collagens—Structure, functions and biosynthesis. *Advanced Drug Delivery Reviews*, *55*, 1531–1546.
Gorham, S. D. (1991). Collagen. In D. Byrom (Ed.), *Biomaterials* (pp. 55–122). New York (NY): Stockton Press.
Gunatillake, A. P., & Adhikari, R. (2003). Biodegradable synthetic polymers for tissue engineering. *European Cells and Material*, *5*, 1–13.
Hori, T., Zhang, H. S., & Shimizu, T. (1988). Changes of water state in acrylic fibers and their glass transition temperature by DSC measurement. *Textile Research Journal*, *58*, 227–232.
Hubbell, J. A. (1995). Biomaterials in tissue engineering. *Nature Biotechnology*, *13*, 565–575.
Kabir, I. G., Yagen, B., Penhasi, A., & Rubinstein, A. (1998). Low swelling, crosslinked guar and its potential use as colon-specific drug carrier. *Pharmaceutical Research*, *15*, 1019–1025.
Kaminska, A., & Sionkowska, A. (1996). Effect of UV radiation on the infrared spectra of collagen. *Polymer Degradation and Stability*, *51*, 19–26.
Laurencin, C. T., Ambrosto, A. M. A., Borden, M. D., & Cooper, J. A. (1999). Tissue engineering: Orthopedic applications. *Annual Review of Biomedical Engineering*, *1*, 19–46.
Marion, M., Monica, A. F. L. M., & Muller, W. D. (2008). Biomaterial interface investigated by electrochemical impedance spectroscopy. *Advanced Engineering Materials*, *10*, B33–B46.
Marzec, E., & Warchol, W. (2005). Dielectric properties of a protein–water system in selected animal tissues. *Bioelectrochemistry*, *65*, 89–94.
Murphy, C. M., Haugh, G., & O'Brien, F. J. (2010). The effect of mean pore size on cell attachment, proliferation and migration in collagen glycosaminoglycan scaffolds for tissue engineering. *Biomaterials*, *31*(3), 461–466.
Obriena, F. J., Harley, B. A., Yannas, I. V., & Gibson, L. J. (2005). The effect of pore size and structure on cell adhesion in collagen–GAG scaffolds. *Biomaterials*, *26*, 433–441.
Ohya, S., & Matsuda, T. J. (2005). Poly (N-isoproylacrylamide) (PNIPAM)-grafted gelatin as thermo responsive three dimensional artificial extracellular matrix: Molecular and formulation parameter vs. cell proliferation potential. *Journal of Biomaterial Science Polymer Edition*, *16*, 809–827.
Panariello, G., Favaloro, R., Forbicioni, M., Caputo, E., & Barbucci, R. (2008). Synthesis of a new hydrogel, based on guar gum for controlled drug release. *Macromolecular Symposium*, *266*, 68–73.
Pethig, R., & Kell, D. B. (1987). The passive electrical properties of biological systems: Their significance in physiology, biophysics and biotechnology. *Physics in Medicine and Biology*, *32*, 933–970.
Rana, M., Nath, L. K., Haque, A., Maity, T., Choudhury, P. K., Shrestha, B., et al. (2010). Formulation and in vitro evaluation of natural polymers based microspheres for colonic drug delivery. *International Journal of Pharmacy and Pharmaceutical Sciences*, *2*, 212–219.
Remi, P. B., Robert, G., & Francois, B. (2010). Collagen-based biomaterials for tissue engineering applications. *Materials*, *3*, 1863–1887.
Rubinstein, A. (2000). Natural polysaccharides as targeting tools of drugs to the human colon. *Drug Delivery Research*, *50*, 435–439.
Samouillan, V., Lamure, A., & Lacabanne, C. (2000). Dielectric relaxations of collagen and elastin in the dehydrated state. *Chemical Physics*, *255*, 259–271.
Samouillan, V., Lamure, A., Maurel, E., Dandurand, J., Lacabanne, C., Ballarin, F., et al. (2000). Characterisation of elastin and collagen in aortic bioprothese. *Medical & Biological Engineering & Computing*, *38*, 226–231.
Singh, B. N., & Kim, K. H. (2005). Effects of divalent cations on drug encapsulation efficiency of deacylated gellan gum. *Journal of Microencapsulation*, *22*, 761–771.
Sionkowska, A. (2000). Modification of collagen films by ultraviolet irradiation. *Polymer Degradation and Stability*, *68*, 147–151.
Van Tienen, T. G., Heijkants, R. G. J. C., Buma, P., De Groot, J. H., Pennings, A. J., & Veth, R. P. H. (2002). Tissue ingrowth and degradation of two biodegradable porous polymers with different porosities and pore sizes. *Biomaterials*, *23*(8), 1731–1738.
Wake, M. C., Patrick, C. W., Jr., & Mikos, A. G. (1994). Pore morphology effects on the fibrovascular tissue growth in porous polymer substrates. *Cell Transplantation*, *3*(4), 339–343.
Woessner, J. F. (1961). The determination of hydroxyproline in tissue and protein samples containing small portions of this imino acid. *Archives of Biochemistry and Biophysics*, *93*, 440–447.
Wolfgang, F. (1998). Collagen—Biomaterial for drug delivery. *European Journal of Pharmaceutics and Biopharmaceutics*, *45*, 113–136.
Yamauchi, T., & Murakami, K. J. (1991). Differential scanning calorimetry as an aid for investigating the wet state pulp. *Journal of Pulp and Paper Science*, *17*, 223–226.